



# Highly dispersed nanocrystallines WC supported on microwave exfoliated RGO by ionic liquid and its catalytic performance in electroreduction of nitrobenzene

Weiming Liu, Meiqin Shi, Xiaoling Lang, Di Zhao, Youqun Chu, Chun'an Ma\*

State Key Laboratory Breeding Base of Green Chemistry-Synthesis Technology, School of Chemical Engineering and Materials Science, Zhejiang University of Technology, Hangzhou 310014, Zhejiang, PR China

## ARTICLE INFO

### Article history:

Received 5 April 2012

Received in revised form 9 August 2012

Accepted 16 August 2012

Available online 18 September 2012

### Keywords:

Tungsten carbide

Reduced graphene oxide

Ionic liquid

Microwave

Nitrobenzene

Electroreduction

## ABSTRACT

Tungsten carbide (WC) nanocrystallines were loaded onto the surface of microwave-exfoliated reduced graphene oxide (RGO) using program-controlled reduction–carbonization technique and modified impregnation method in the presence of ionic liquid (IL). The characterization results show that WC nanocrystallines with a size of ca.80 nm were highly dispersed on RGO with the assistance of IL. The electrocatalytic activity of the prepared WC/RGO (IL) was evaluated in the nitrobenzene reduction reaction. It was found that the WC/RGO (IL) gave better activity and stability than single RGO or WC/RGO that were prepared in the absence of IL. The high activity of WC/RGO (IL) can be explained to be the result of the synergistic function between WC and RGO. It was also proved that the pre-treatment of GO by microwave-exfoliated method was an effective way to form the graphene-based intercalation materials. Our study demonstrated that WC/RGO (IL) could be a promising alternative catalyst toward the nitrobenzene electroreduction because of its higher performance and lower cost.

© 2012 Elsevier B.V. All rights reserved.

## 1. Introduction

Nitrobenzene is widely used in the chemical production, such as aniline, aniline dyes, explosives, pesticides and drugs, and also acts as a solvent in products like paints, shoes and floor metal polishes [1]. However, nitrobenzene has been understood as a great threat to human health and environment because of its high toxicity [2,3]. The strong electron affinity of nitro reduces the electron cloud density of benzene ring and thus makes nitrobenzene very stable. It is urgent to explore the efficient ways to degrade nitrobenzene. Nitrobenzene electroreduction has recently aroused increasing interest because of its cleaner process [4], which plays an important role in industries. Therefore, the novel cathodic electrocatalytic material with better activity and lower cost for the electroreduction of nitrobenzene is highly desirable.

In the past two decades, our group has been studying WC and its composites because of its “platinum-like” behavior in surface catalysis [5] and its strong resistance to corrosion and catalytic poisons. WC has lower hydrogen overpotential and offers stronger hydrogen adsorption capacity which means to be the suitable electrocatalyst in the electroreduction. Additionally, WC was reported as a promising material to replace noble catalyst (such as platinum) in alkane reforming and alkane isomerization [6–9]. Therefore, WC is

also expected to show better performance toward the nitrobenzene electroreduction. In our early work, we investigated WC and WC/CNTs electrodes in the nitrobenzene electroreduction. The results proved that WC had the good electrocatalytic activity toward nitrobenzene reduction. Moreover, WC/CNTs showed better performance in comparison with the case of pure WC or CNTs, which is ascribed to the superior surface effect of CNTs and good dispersion of WC on CNTs. Hence, more inspiring results on WC composites can be achieved if the suitable supports and effective synthesis ways are found to enhance the entire distribution of WC on the support and improve its electronic property.

Graphene, a single-atom-thick planar sheet of hexagonally arrayed  $sp^2$  hybridized carbon, which is the basis of carbon nanotubes and graphite, has attracted tremendous attention in nanoscience because of its strictly two-dimension and its outstanding electronic, thermal and mechanical properties [10–13]. It exhibits promising potential application in many technological fields, such as nanoelectronics, sensors, nanocomposites, batteries, supercapacitors and hydrogen storage [10], especially as a new catalyst support to enhance electrocatalytic activity [14–17]. At present, chemically converted graphene, which is prepared typically from graphite oxide (GO) or graphene oxide (GO) with different reductants, is commonly named as reduced graphene oxide (RGO). RGO is superior compared to CNTs, such as lower production cost, higher available surface area, and being easily obtained by chemical conversion of inexpensive GO [14]. Meanwhile, besides being the support, RGO also can be used as a catalyst for

\* Corresponding author. Tel.: +86 571 88320830; fax: +86 571 88320830.  
E-mail address: [science@zjut.edu.cn](mailto:science@zjut.edu.cn) (C. Ma).

hydrogenation of nitrobenzene [18]. Therefore, much higher electrocatalytic activity can, in principle, be achieved by the introduction of WC onto a RGO support.

In this study, precursor GO was exfoliated by microwave irradiation to obtain the high-specific area support. WC/RGO (IL) was prepared by depositing highly dispersed WC nanocrystallines on the support using program-controlled reduction–carbonization technique and modified impregnation method in the presence of ionic liquid (IL). Compared with other common processes, the procedure used in our study for preparing the WC/RGO (IL) has several advantages: (1) under microwave irradiation, the pristine GO powders were expanded and exploded rapidly to result in a porous structure and larger interlayer spaces, which constituted a framework for tungsten-containing groups to infiltrate into the interlayers of GO; (2) ethanol was used as the solvent, and GO can be easily dispersed in ethanol because of its hydrophilicity; (3) in  $\text{WCl}_6$ , the source of WC in our processes, W end of the bond is positive and the Cl end is negative because Cl is more electronegative than W, while the one end of IL ([BMIM][PF6]) is  $[\text{PF}_6]^-$  which can bond with atom W. On the other hand, the another end of IL,  $[\text{BMIM}]^+$ , has the tendency to move forward to the interlayers of GO which are negatively charged due to the oxygenated groups such as hydroxyl and carboxyl groups. In this way, the tungsten-containing groups will be anchored tightly on the surfaces of GO. As discussed above, the presence of IL facilitated the self-assemble process to obtain the highly dispersed precursor tungsten-containing groups/GO.

## 2. Experimental

### 2.1. Synthesis of graphite oxide (GO)

GO was derived from graphite powders (SP, from sinopharm chemical reagent Co., Ltd.) with a modified Hummers method which was originally presented by Kovtyukhova et al. [19,20]. Graphite and  $\text{KMnO}_4$  powders were mixed in concentrated  $\text{H}_2\text{SO}_4$  (23 mL) under constant stirring at ca.  $10^\circ\text{C}$  for 2 h. After the mixture was stirred at ca.  $35^\circ\text{C}$  for 30 min, deionized (DI) water was slowly added to the beaker and the oxidation reaction proceeded at ca.  $98^\circ\text{C}$  for 1 h. The reaction was ended by adding DI water followed by 30%  $\text{H}_2\text{O}_2$  solution so as to neutralize redundant  $\text{KMnO}_4$ . Finally, the mixture was centrifugated and washed with DI water several times, and then the obtained mixture was dried in an air oven at  $80^\circ\text{C}$ .

### 2.2. Pretreatment of GO

The as-prepared GO powders were sealed in a microwave kettle and treated in a microwave apparatus Initiator EXP EU (Biotage, Sweden) in ambient conditions at  $110^\circ\text{C}$ .

### 2.3. Synthesis of WC/RGO

Solution A: tungsten hexachloride ( $\text{WCl}_6$ ) was added to a beaker, mixed with 1 mL of [BMIM][PF6] (Lanzhou Greenchem ILS, LICP, CAS, China) and 40 mL of ethanol. Solution B: after microwave irradiation, the GO powders were dispersed in ethanol. Subsequently, solution A was added to solution B and the mixture was heated to remove the ethanol, then centrifugated and dried at  $70^\circ\text{C}$  to form a precursor. The as prepared precursor was carbonized in a tubal resistance furnace. Firstly, the furnace was purified with  $\text{N}_2$  for 30 min to remove the air. The obtained precursor was subsequently preserved at  $900^\circ\text{C}$  for a few hours with the gas of CO and  $\text{H}_2$ . The fabrication procedure of WC/RGO was demonstrated in Fig. 1. For comparison, RGO without loading WC obtained by direct

carbonization and WC/RGO synthesized in the absence of ionic liquid were also prepared, denoted as RGO and WC/RGO respectively.

### 2.4. Sample characterization

$\text{N}_2$  adsorption–desorption was examined by ASAP 2020 (Micromeritics, America) and the specific surface area of GO was measured by Brunauer–Emmett–Teller (BET) method. The morphologies of the samples were observed by SEM Hitachi S-4700 II (Hitachi, Japan), using  $\text{Cu K}\alpha$  radiation ( $\lambda = 0.154\text{ nm}$ ). The crystalline structures were investigated by X-ray diffraction (XRD) with an X'Pert PRO X-ray (PANalytical, Netherlands) at room temperature.  $\text{Cu K}\alpha$  radiation (40 kV, 40 mA) was applied and an angle range from  $10^\circ$  to  $80^\circ$  was recorded at 0.05 increments. Transmission electron microscopy (TEM) was performed with a Tecnai G2 F30 S-Twin microscope (FEI, Netherlands), coupled with energy dispersive X-ray spectrometer (EDX, Thermo NORAN VANSTAGE ESI), also using  $\text{Cu K}\alpha$  radiation. The element distribution of the powders was characterized by EDX.

### 2.5. Electrochemical measurements

The electrochemical measurement of the samples was performed in a conventional three electrode system. The reference electrode, counter electrode, and working electrode were saturated calomel electrode (SCE), Pt plate ( $2\text{ cm}^2$ ) and glassy carbon disk (3 mm in diameter), respectively. All the electrochemical experiments were carried out using the CHI 660d electrochemical workstation (Cheng-Hua, Shanghai, China) at room temperature. The working electrodes were composed of the WC/RGO (IL) powders deposited as an ultra-thin layer on an activated glassy carbon disk, 5 mm diameter. WC/RGO (IL) was suspended in ethanol containing 5 wt% Nafion solution (Ruibang New Energy Technology Co., Ltd., China) under ultrasonication for 30 min. A  $20\ \mu\text{L}$  of the suspension was pipette on top of the glassy carbon disk electrode and then dried in infrared desiccators to form the ultra-thin layer. WC/RGO and RGO electrodes were prepared by the same process. The aqueous solutions containing  $0.5\text{ mol L}^{-1}\ \text{H}_2\text{SO}_4$  with or without  $5\text{ mmol L}^{-1}$  nitrobenzene were used as electrolytes, which were purged with highly purified nitrogen for 30 min prior to electrochemical measurement, and all experiments were carried out at room temperature.

## 3. Results and discussion

### 3.1. Exfoliation of GO by microwave irradiation

GO was exfoliated by microwave irradiation. Fig. 2(a) and (b) are  $\text{N}_2$  adsorption–desorption isotherms of GO before and after microwave treatment, obviously both the samples are characterized by type II isotherms and possess hysteresis loops of type H3. According to the prescription of IUPAC, the type II isotherm indicates that there are no micropores or large mesopores in the samples and the type H3 hysteresis loop at relatively high pressure suggests that there exist asymmetrically slit-shaped pores with large pore size. Nevertheless, it is interesting to note that after microwave treatment the adsorption of  $\text{N}_2$  on GO, is enhanced comparing Fig. 2(b) with (a) at the same  $P/P_0$ , and the BET values of the samples are  $13.6$  and  $79.8\text{ m}^2/\text{g}$  respectively as seen in Fig. 2(a) and (b). Under microwave irradiation, the pristine GO powders which were heated in short time expanded and exploded rapidly. A great amount of large pores were constituted because of the release of adsorbed water existing in interlayers and partial decomposition of the oxygen-containing groups (epoxide, hydroxyl, carboxyl, carbonyl groups). Thus after microwave exfoliation, the

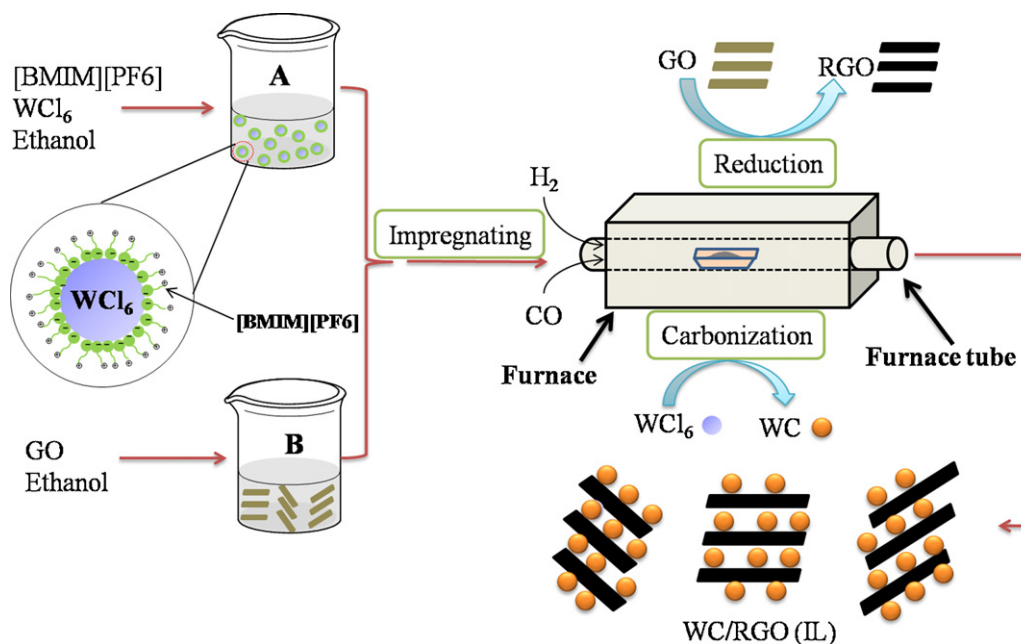


Fig. 1. Schematic illustration shows synthesis of WC/RGO (IL) composites.

specific surface area of GO was increased compared with the samples prepared by normal Hummers method, which is the reason why the microwave pretreated GO possessed higher adsorption quantity.

Fig. 3 is the SEM images showing the difference of the morphologies of GO before and after microwave irradiation. In Fig. 3(a), GO obtained by the normal Hummers method shows a tightly stack between graphite layers, while GO powders after microwave irradiation in Fig. 3(b) were exfoliated to a very large extent and has "a wave-like" morphology [21–24]. Upon microwave irradiation, the volume and interlayer space of the GO powders expand rapidly because of 'violent fuming' [25], thereby causes a larger specific surface area which matches with the BET results. Moreover, the increase of the interlayer space is applicable to the total immersion of GO in the solvent and the subsequent assembling of active components.

### 3.2. Characterization of catalysts

Fig. 4 gives the XRD patterns of the three samples. The peaks at the  $2\theta$  of 26.53° and 43.06° with the d-spacing values of 3.36 and 2.10 are corresponding to the (002) and (100) facets of RGO [17], the  $2\theta$  of 31.36°, 35.53°, 48.23°, 64.14°, 65.56°, 73.06°, 75.06° and 76.93° with the d-spacing values of 2.85, 2.52, 2.28, 1.45, 1.42, 1.29, 1.26 and 2.10 are corresponding to the (001), (100), (101), (110), (002), (111), (200) and (102) facets of WC [26–28]. As shown in Fig. 4b, the typical diffraction peak (001) of GO disappears while the typical diffraction peak (002) of RGO enhances after reduction by H<sub>2</sub>. It could be concluded that GO sheets were effectively reduced to graphene and restacked into an ordered graphite crystalline structure via program-controlled reduction–carbonization technique. In Fig. 4(a) and (b), the three typical diffraction peak (001), (100), and (101) of WC can be observed, which

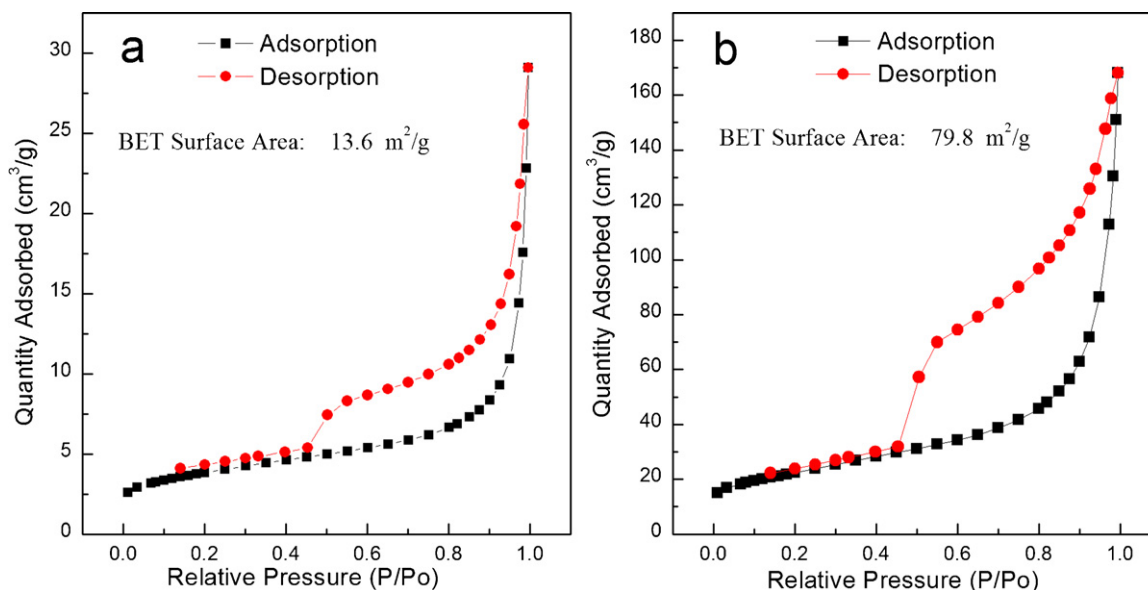


Fig. 2. N<sub>2</sub> adsorption–desorption isotherms of GO (a) before and (b) after treatment by microwave irradiation.

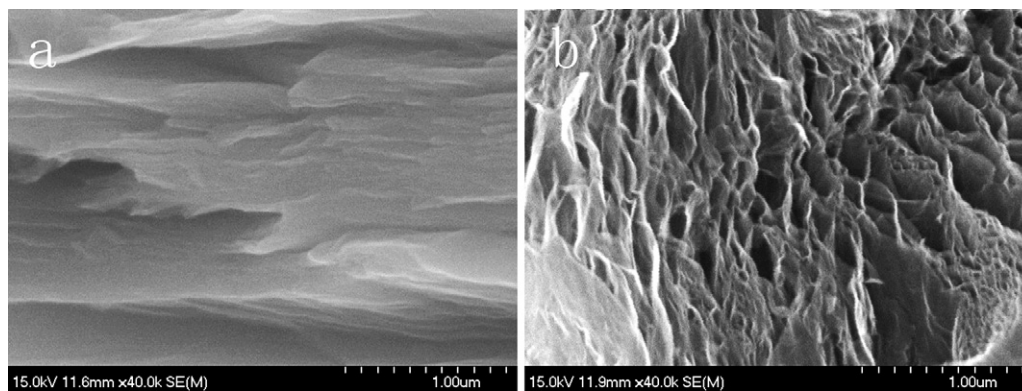


Fig. 3. SEM images of GO (a) before (b) after microwave irradiation.

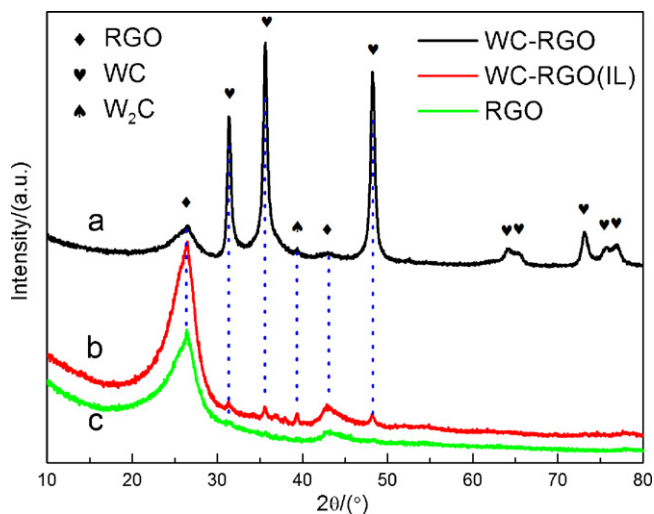


Fig. 4. The XRD patterns of (a) WC/RGO, (b) WC/RGO (IL) and (c) RGO.

indicates that WC nanocrystallines were loaded on RGO successfully. However, a small quantity of W<sub>2</sub>C can also be found in both samples, probably because of the incomplete carbonization of WCl<sub>6</sub>.

Ionic liquid (IL), a kind of room temperature organic salts, has been widely used as a new reaction medium due to its unique properties such as low volatility, good thermal stability, good dissolving ability, high ion conductivity and wide electrochemical window [29–33]. In this work we prepared WC/RGO (IL) in the presence of IL ([BMIM][PF6]). Fig. 5(a) and (b) are

the images of RGO supported WC nanocrystallines synthesized with and without IL. It can be seen in Fig. 5(a) that the WC nanocrystallines, the bright particles, in the sample of WC/RGO aggregate together and distribute mainly on the edges of RGO sheets with a size of around 130 nm. In Fig. 5(b), different from the previous figure, the WC nanocrystallines in the sample of WC/RGO (IL) deposited on both sides and edges of RGO sheets with a smaller size and higher dispersion. This could be attributed to the use of IL in the synthesis progress. WO species, generated from WCl<sub>6</sub>, can anchor on the interlayers of RGO uniformly with the existence of IL. So that the nucleation of nanocrystallines was dispersed efficiently and the growing of crystallines was also hindered because the interaction of IL will make great impact on the nucleation and growth of nanocrystallines [34].

Fig. 6 shows the typical TEM images and the corresponding EDX patterns of WC/RGO and WC/RGO (IL). The similar results were confirmed in the aspect of distribution and particles size, which suggested that the IL played an important role in controlling particle size of WC and preventing them from aggregation.

### 3.3. Electrochemical measurements of the samples

The electrocatalytic activity of WC/RGO, WC/RGO (IL) and RGO electrodes toward nitrobenzene electroreduction were evaluated in 0.5 mol L<sup>-1</sup> H<sub>2</sub>SO<sub>4</sub> with 5 mmol L<sup>-1</sup> nitrobenzene using CV, as shown in Fig. 7. It was reported [4,35] that the procedure of the nitrobenzene electroreduction reaction in acid medium could be expressed as follows.

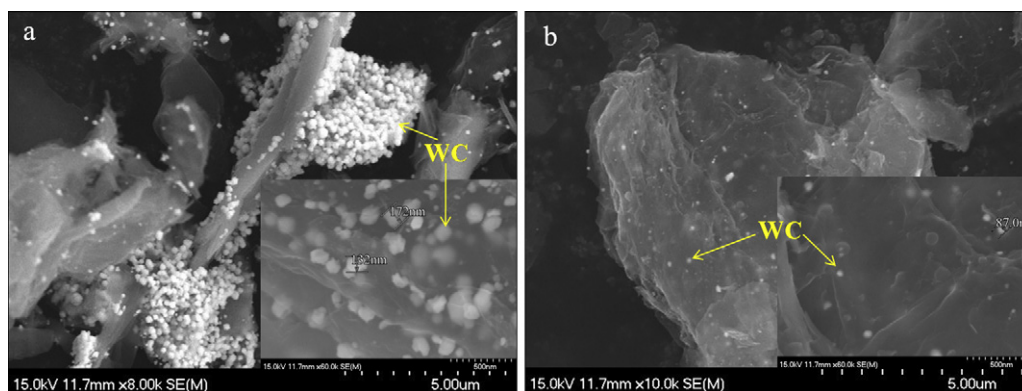
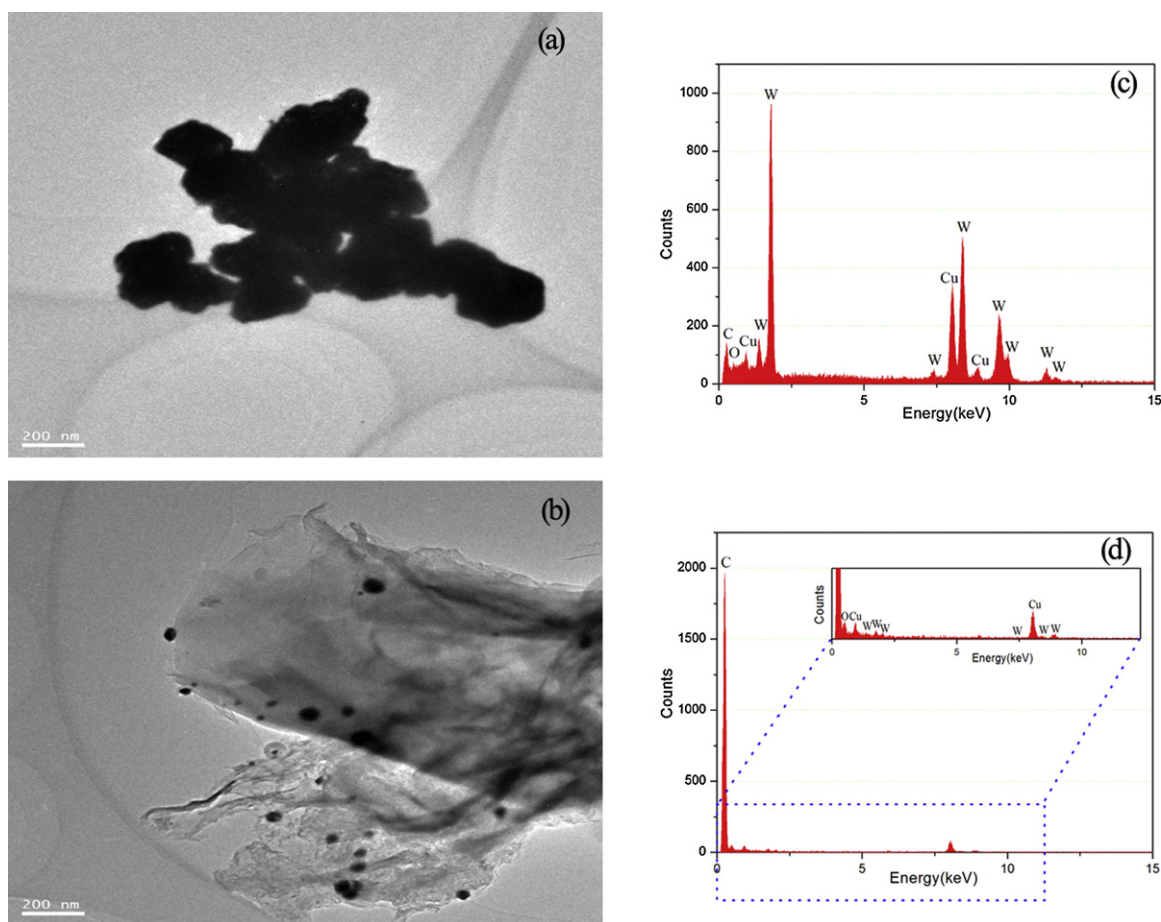
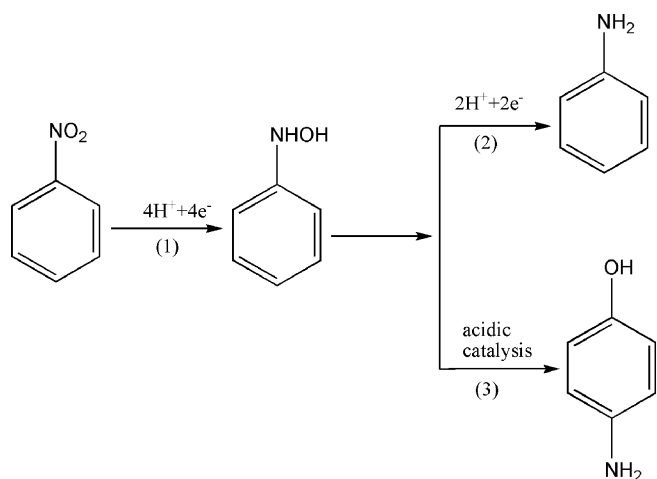


Fig. 5. SEM images of GO (a) WC/RGO and (b) WC/RGO (IL). The insets are their SEM images in high magnification.



**Fig. 6.** TEM image of GO (a) WC/RGO and (b) WC/RGO (IL). The corresponding EDX patterns of (c) WC/RGO and (d) WC/RGO (IL).



The nitrobenzene first diffuses onto the electrode and is reduced to phenylhydroxylamine (PHA) by the four-electron at the potential range of  $-0.6$  to  $-0.2$  V (reaction (1)). Consequently PHA continues to be reduced to aniline by the two-electron at the potential of ca.  $-0.8$  V (reaction (2)) or diffuses into the solution to produce p-aminophenol by rearrangement (reaction (3)). Compared with the literature data, the main reaction in our test is the reduction of nitrobenzene to PHA corresponding to the main reduction peak at ca.  $-0.35$  V in Fig. 7. The inset of Fig. 7, is the CV curves of the WC/RGO, WC/RGO (IL) and RGO electrodes in  $0.5 \text{ mol L}^{-1} \text{ H}_2\text{SO}_4$ , provides the background information for the electrochemical processes taking place on the catalysts surfaces. There is no current peak except for the hydrogen evolution peaks

when the three prepared samples were tested in  $0.5 \text{ mol L}^{-1} \text{ H}_2\text{SO}_4$ . After adding the nitrobenzene into  $\text{H}_2\text{SO}_4$ , the irreversible cathodic current peaks appeared at  $-0.345$  V,  $-0.333$  V and  $-0.334$  V respectively in the three samples, and the corresponding data are listed in Table 1. Compared with those of WC/RGO and RGO, the cathodic peak potential of WC/RGO (IL) shifted positively for ca. 12 mV and 1 mV. Furthermore, it can be observed from Fig. 7 and Table 1 that the onset potentials of nitrobenzene electroreduction on WC/RGO (IL) are more positive than those on WC/RGO and RGO.

The catalytic currents are calculated for per unit mass which refers to the total film on GC surface. The currents observed on CV curves of WC/RGO and WC/RGO (IL) are 1.64 and 1.95 mA/mg, higher than the value of 0.34 mA/mg, obtained from RGO (Table 1). Based on Randles–Sevcik equation, the peak currents are proportional to the area of the electroactive surface area [3]. So the electroactive surface area for WC/RGO (IL) electrode is larger than those of the other two. According to early works, RGO can be used as a catalyst for hydrogenation of nitrobenzene [21]. The change

**Table 1**

Comparison of different electrocatalytic activity parameters from the cyclic voltammetry of nitrobenzene electrochemical reduction among the prepared WC/RGO, WC/RGO (IL) and RGO catalysts.

Samples	$i_p^a$ (mA/mg mass)	$E_p^b$ (V vs. SCE)	Onset potential (V vs. SCE)
WC/RGO (IL)	1.95	$-0.333$	$-0.243$
WC/RGO	1.64	$-0.345$	$-0.261$
RGO	0.34	$-0.334$	$-0.246$

<sup>a</sup> Peak current.

<sup>b</sup> Peak potential.

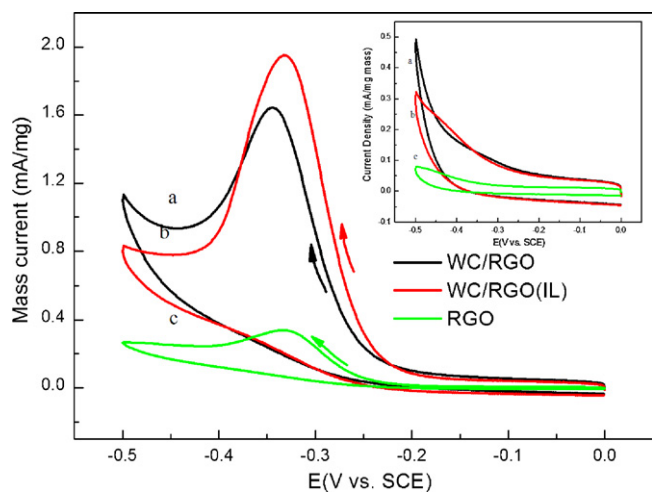
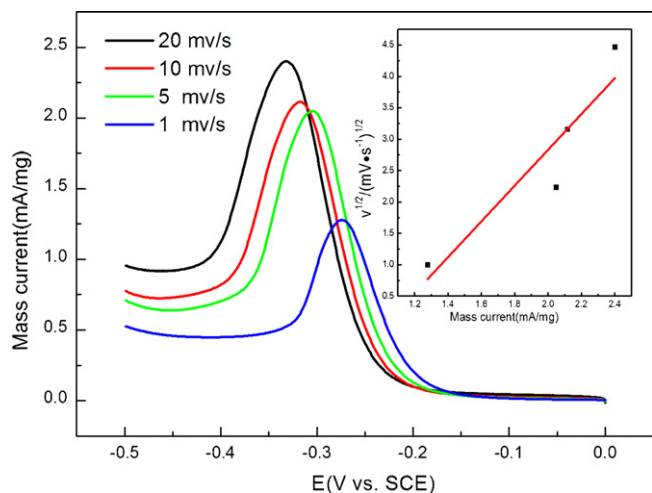


**Fig. 7.** The cyclic voltammograms (CV) of (a) WC/RGO, (b) WC/RGO (IL) and (c) RGO electrocatalysts tests in  $0.5 \text{ mol L}^{-1} \text{ H}_2\text{SO}_4 + 5 \text{ mmol L}^{-1}$  nitrobenzene at a scan rate of  $20 \text{ mV s}^{-1}$  at room temperature. The inset is the CV curves of the same electrocatalysts in  $0.5 \text{ mol L}^{-1} \text{ H}_2\text{SO}_4$  solution.

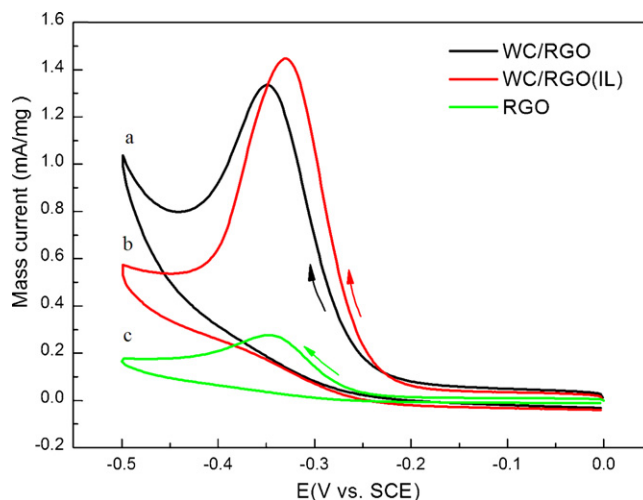
in the current density demonstrates that the improved reaction kinetics of nitrobenzene reduction on WC/RGO (IL) and WC/RGO catalysts may due to synergistic effect between WC and RGO. The results above indicate that all the three samples exhibit electrocatalytic activity toward the reduction of nitrobenzene, but WC/RGO (IL) electrode performs best. The greatly enhanced electrochemical behavior of WC/RGO (IL) may be attributed to its smaller size and more uniformly dispersed on the surfaces of RGO.

Fig. 8 presents the Linear Sweep Voltammetry (LSV) of WC/RGO (IL) electrode in  $0.5 \text{ mol L}^{-1} \text{ H}_2\text{SO}_4 + 5 \text{ mmol L}^{-1}$  nitrobenzene at different scan rate at room temperature. The plot of peak currents vs. square root of scan rate is given in the inset. A nearly linear dependence is found on the WC/RGO (IL) electrode (Fig. 8), suggesting that the electrode reaction is controlled by the diffusion.

The CV curves of the same samples after 400 cycles are shown in Fig. 9. It is clear that all the peak current densities decrease for nitrobenzene reduction on three catalysts. However, WC/RGO (IL) still illustrates the highest current peak and the results are listed in Table 2. Moreover, both before and after 400 cycles, the onset potential of the nitrobenzene electroreduction on WC/RGO (IL)



**Fig. 8.** The Linear Sweep Voltammetry (LSV) of WC/RGO (IL) electrocatalysts tests in  $0.5 \text{ mol L}^{-1} \text{ H}_2\text{SO}_4 + 5 \text{ mmol L}^{-1}$  nitrobenzene at different scan rate at room temperature. The inset is the plot of peak currents vs. square root of scan rate.



**Fig. 9.** The cyclic voltammograms (CV) of (a) WC/RGO, (b) WC/RGO (IL) and (c) RGO electrocatalysts tests in  $0.5 \text{ mol L}^{-1} \text{ H}_2\text{SO}_4 + 5 \text{ mmol L}^{-1}$  nitrobenzene at a scan rate of  $20 \text{ mV s}^{-1}$  at room temperature after 400 cycles.

**Table 2**

Comparison of different electrocatalytic activity parameters from the cyclic voltammetry of nitrobenzene electrochemical reduction after 400 cycles between the prepared WC/RGO, WC/RGO (IL) and RGO catalysts.

Samples	$i_p^a$ (mA/mg mass)	$E_p^b$ (V vs. SCE)
WC/RGO (IL)	1.45	-0.329
WC/RGO	1.34	-0.349
RGO	0.28	-0.346

<sup>a</sup> Peak current.

<sup>b</sup> Peak potential.

catalyst is the most positive value, compared with those of the other two. The results reconfirmed that toward the nitrobenzene electroreduction, WC/RGO (IL) gave the best performance.

#### 4. Conclusions

In summary, WC/RGO (IL) was successfully synthesized using program-controlled reduction-carbonization technique and modified impregnation method in the presence of ionic liquid (IL). IL was used as dispersing agent to prepare the WC nanocrystallines with smaller size and better distribution. Compared to the RGO and WC/RGO catalyst, the WC/RGO (IL) displayed better stability and higher electrocatalytic activity toward nitrobenzene reduction reaction, showing a significantly lower overpotential and a higher peak current. The WC/RGO (IL) catalyst could be a promising alternative catalyst for nitrobenzene electroreduction because of its higher activity and lower preparing cost. Meanwhile, our method used in this work for preparing WC/RGO (IL) also set an example for synthesis of other carbide compounds supported on RGO.

#### Acknowledgement

This work was supported by International Science & Technology Cooperation Program of China (2010DFB63680), Key Project of Natural Science Foundation of Zhejiang Province (Z4100790), Science and Technology Program of Zhejiang Province (2011R09002-08), the 973 Project from the Ministry of Science and Technology of China (2012CB722604), and Science and Technology Major Project in International Cooperation of Zhejiang Province (2008C14040).

#### References

- [1] A. Latifoglu, M.D. Gurol, Water Research 37 (2003) 1879.

- [2] D.S. Bhatkhande, V.G. Pangarkar, A.A.C.M. Beenackers, *Water Research* 37 (2003) 1223.
- [3] B. Qi, F. Lin, J. Bai, L. Liu, L. Guo, *Materials Letters* 62 (2008) 3670.
- [4] Y.-P. Li, H.-B. Cao, C.-M. Liu, Y. Zhang, *Journal of Hazardous Materials* 148 (2007) 158.
- [5] H. Böhm, *Journal of Power Sources* 1 (1976) 177.
- [6] H.H. Hwu, J.G. Chen, K. Kourtakis, J.G. Lavin, *The Journal of Physical Chemistry B* 105 (2001) 10037.
- [7] V. Keller, P. Wehrer, F. Garin, R. Ducros, G. Maire, *Journal of Catalysis* 153 (1995) 9.
- [8] C. Moreno-Castilla, M.A. Alvarez-Merino, F. Carrasco-Marín, J.L.G. Fierro, *Langmuir* 17 (2001) 1752.
- [9] J.B.O. Santos, G.P. Valença, J.A.J. Rodrigues, *Journal of Catalysis* 210 (2002) 1.
- [10] A.K. Geim, K.S. Novoselov, *Nature Materials* 6 (2007) 183.
- [11] D. Li, R.B. Kaner, *Science* 320 (2008) 1170.
- [12] K.S. Novoselov, A.K. Geim, S.V. Morozov, D. Jiang, Y. Zhang, S.V. Dubonos, I.V. Grigorieva, A.A. Firsov, *Science* 306 (2004) 666.
- [13] S. Stankovich, D.A. Dikin, G.H.B. Dommett, K.M. Kohlhaas, E.J. Zimney, E.A. Stach, R.D. Piner, S.T. Nguyen, R.S. Ruoff, *Nature* 442 (2006) 282.
- [14] Y. Li, W. Gao, L. Ci, C. Wang, P.M. Ajayan, *Carbon* 48 (2010) 1124.
- [15] R. Muszynski, B. Seger, P.V. Kamat, *The Journal of Physical Chemistry C* 112 (2008) 5263.
- [16] Y. Si, E.T. Samulski, *Chemistry of Materials* 20 (2008) 6792.
- [17] G. Williams, B. Seger, P.V. Kamat, *Acs Nano* 2 (2008) 1487.
- [18] Y. Gao, D. Ma, C. Wang, J. Guan, X. Bao, *Chemical Communications* 47 (2011) 2432.
- [19] J.W.S. Hummers, R.E. Offeman, *Journal of the American Chemical Society* 80 (1958) 1339.
- [20] N.I. Kovtyukhova, P.J. Ollivier, B.R. Martin, T.E. Mallouk, S.A. Chizhik, E.V. Buzaneva, A.D. Gorchinskiy, *Chemistry of Materials* 11 (1999) 771.
- [21] D.D.L. Chung, *Journal of Materials Science* 22 (1987) 4190.
- [22] E.H.L. Falcao, R.G. Blair, J.J. Mack, L.M. Viculis, C.-W. Kwon, M. Bendikov, R.B. Kaner, B.S. Dunn, F. Wudl, *Carbon* 45 (2007) 1367.
- [23] O.Y. Kwon, S.W. Choi, K.W. Park, Y.B. Kwon, *Journal of Industrial and Engineering Chemistry* 9 (2003) 743.
- [24] B. Tryba, A.W. Morawski, M. Inagaki, *Carbon* 43 (2005) 2417.
- [25] Y. Zhu, S. Murali, M.D. Stoller, A. Velamakanni, R.D. Piner, R.S. Ruoff, *Carbon* 48 (2010) 2118.
- [26] H. Chhina, S. Campbell, O. Kesler, *Journal of Power Sources* 164 (2007) 431.
- [27] R. Ospina, P. Arango, Y.C. Arango, E. Restrepo, A. Devia, *Physica Status Solidi C* 2 (2005) 3758.
- [28] N.J. Welham, *AIChE Journal* 46 (2000) 68.
- [29] H. Hu, H. Yang, P. Huang, D. Cui, Y. Peng, J. Zhang, F. Lu, J. Lian, D. Shi, *Chemical Communications* 46 (2010) 3866.
- [30] D.-W. Kim, D.-K. Kim, M.-I. Kim, D.-W. Park, *Catalysis Today* 185 (2012) 217.
- [31] B. Zhang, W. Ning, J. Zhang, X. Qiao, J. Zhang, J. He, C.-Y. Liu, *Journal of Materials Chemistry* 20 (2010) 5401.
- [32] H. Zhang, X. Li, G. Chen, *Journal of Materials Chemistry* 19 (2009) 8223.
- [33] X. Zhou, T. Wu, B. Hu, G. Yang, B. Han, *Chemical Communications* 46 (2010) 3663.
- [34] J. Shen, M. Shi, B. Yan, H. Ma, N. Li, M. Ye, *Nano Research* 4 (2011) 795.
- [35] J. Marquez, D. Pletcher, *Journal of Applied Electrochemistry* 10 (1980) 567.